Transp Porous Med (2012) 93:431–451
DOI 10.1007/s11242-012-9961-8

Predicting Tortuosity for Airflow Through Porous Beds Consisting of Randomly Packed Spherical Particles

Wojciech Sobieski · Qiang Zhang · Chuanyun Liu

Received: 1 December 2010 / Accepted: 8 February 2012 / Published online: 2 March 2012

Abstract This article presents a numerical method for determining tortuosity in porous beds consisting of randomly packed spherical particles. The calculation of tortuosity is carried out in two steps. In the first step, the spacial arrangement of particles in the porous bed is determined by using the discrete element method (DEM). Specifically, a commercially available discrete element package (PFC^{3D}) was used to simulate the spacial structure of the porous bed. In the second step, a numerical algorithm was developed to construct the microscopic (pore scale) flow paths within the simulated spacial structure of the porous bed to calculate the lowest geometric tortuosity (LGT), which was defined as the ratio of the shortest flow path to the total bed depth. The numerical algorithm treats a porous bed as a series of four-particle tetrahedron units. When air enters a tetrahedron unit through one face (the base triangle), it is assumed to leave from another face triangle whose centroid is the highest of the four face triangles associated with the tetrahedron, and this face triangle will then be used as the base triangle for the next tetrahedron. This process is repeated to establish a series of tetrahedrons from the bottom to the top surface of the porous bed. The shortest flow path is then constructed geometrically by connecting the centroids of base triangles of consecutive tetrahedrons. The tortuosity values calculated by the proposed numerical method compared favourably with the values obtained from a CT image published in the literature for a bed of grain (peas). The proposed model predicted a tortuosity of 1.15, while the tortuosity estimated from the CT image was 1.14.

Keywords Porous media · Pore structure · Tortuosity · Porosity · Discrete element method

W. Sobieski (✉)
Faculty of Technical Sciences, University of Warmia and Mazury in Olsztyn, M. Oczapowskiego 11, 10-957 Olsztyn, Poland
e-mail: wojciech.sobieski@uwm.edu.pl

Q. Zhang · C. Liu
Department of Biosystems Engineering, University of Manitoba, Winnipeg, MB, Canada
e-mail: zhang@cc.umanitoba.ca

1 Introduction

Studies on fluid flow through porous media were first carried out at least 150 years ago. In 1856, Henry Darcy formulated the first law of flow resistance through porous media (Hellstrm and Lundstrm 2006; Miwa and Revankar 2009):

$$-\frac{\mathrm{d}p}{\mathrm{d}L} = \frac{1}{\kappa} \cdot \mu \cdot \overrightarrow{v}_f, \tag{1}$$

where dL—a segment (m) along which a pressure drop dp (Pa) occurs, κ—permeability coefficient (m^2), μ—dynamic viscosity coefficient (kg/(m s)), $\overrightarrow{v_\mathrm{f}}$—filtration velocity (m/s). The permeability coefficient κ played a key role in determining the pressure drop in Darcy's equation. This coefficient is an intrinsic property of porous media and its value is usually determined experimentally. There exists many formulas that describe the permeability (or filtration coefficient), but they usually produce different results and are difficult to apply in practice. In 1901, Philipp Forchheimer proposed another law applicable to a wider range of flow rates (Andrade et al. 1999; Ewing et al. 1999; Hellstrm and Lundstrm 2006; Miwa and Revankar 2009):

$$-\frac{\mathrm{d}p}{\mathrm{d}L} = \frac{1}{\kappa} \cdot \mu \cdot \overrightarrow{v}_\mathrm{f} + \beta \cdot \rho \cdot \overrightarrow{v}_\mathrm{f}^2, \tag{2}$$

where $\beta\,(1/m)$ is the Forchheimer coefficient (also known as non-Darcy coefficient, or β factor) and ρ is the fluid density (kg/m^3). This law is similar to Darcy's, but it has an additional nonlinear term containing a new coefficient known as the Forchheimer coefficient, β factor, or non-Darcy coefficient. Darcy's and Forchheimer's laws describe flows through porous media on macroscopic level (Bear and Bachmat 1991).

In the literature, there is no consensus on how to select the values of permeability κ and coefficient β in using the Forchheimer equation although many empirical formulas could be found. This problem has attracted the attention of many researchers (e.g. Pazdro and Bohdan 1990; Mian 1992; Skjetne et al. 1999; Samsuri et al. 2003; Sawicki et al. 2004; Belyadi 2006a,b; Lord et al. 2006; Amao 2007; Nałęcz 1991; Mitosek 2007). It is generally agreed that the two coefficients in the Forchheimer equation are functions of the microstructural parameters of the porous media that is:

$$\begin{cases} \frac{1}{\kappa} = f_1(d, e, \phi, ...) \\ \beta = f_2(d, e, \tau, \phi, ...), \end{cases} \tag{3}$$

where d is the particle diameter (m), e is the volumetric porosity coefficient (m^3/m^3), ϕ is the sphericity (–) and τ is the tortuosity (m/m).

In the case of fluid flow through a porous bed consisting of spherical particles, the two coefficients (κ and β) could be determined by the well known Ergun equation (1952) (Niven 2002; Hernndez 2005):

$$-\frac{\mathrm{d}p}{\mathrm{d}L} = \left[\frac{150 \cdot (1-e)^2}{e^3 \cdot (\phi \cdot d)^2}\right] \cdot \mu \cdot \overrightarrow{v}_\mathrm{f} + \left[\frac{1.75 \cdot (1-e)}{e^3 \cdot (\phi \cdot d)}\right] \cdot \rho \cdot \overrightarrow{v}_\mathrm{f}^2. \tag{4}$$

The permeability κ may also be calculated by the Kozeny and Carman equation for well sorted sand (Littmann 2004; Neithalath et al. 2009; Fourie et al. 2007):

$$-\frac{\mathrm{d}p}{\mathrm{d}L} = \left[C_\mathrm{KC} \cdot \tau_\mathrm{f} \cdot S_0^2 \cdot \frac{(1-e)^2}{e^3}\right] \cdot \mu \cdot \overrightarrow{v}_\mathrm{f}, \tag{5}$$

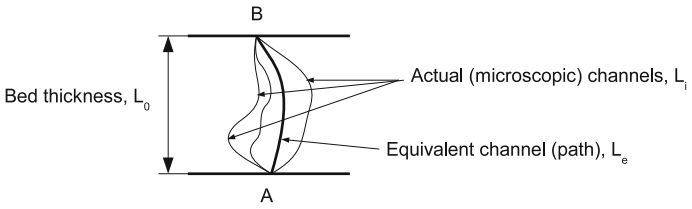

Fig. 1 Geometrical interpretation of the equivalent path

where C_{KC} is a model constant $(1/\mathrm{m}^4)$, τ_f the tortuosity factor $(\mathrm{m}^2/\mathrm{m}^2)$ defined as the square of the tortuosity τ and S_0 is the specific surface of the porous body (m).

It can be seen from the above review of various formulas that there are two intrinsic parameters that affect the flow through porous media: porosity and tortuosity. The porosity can usually be measured easily or calculated theoretically for regularly (ideally) packed particle assemblies, but it has been a long-standing challenge to researchers to experimentally measure or theoretically calculate the tortuosity. When a fluid flows through a porous bed, it moves through connected pores between particles. The ratio of the actual length of flow path to the physical depth of a porous bed is defined as the tortuosity as follows (Lu et al. 2009; Wu et al. 2008):

$$\tau = \frac{L_{\mathrm{e}}}{L_0}, \tag{6}$$

where L_{e} is the length of flow path (m) and L_0 is the depth of porous bed (m).

There is some "ambiguity" in this definition of tortuosity of porous media. When a fluid flows from point A to B in a porous medium, there are more than one possible channels, each a path length L_i (Fig. 1). If tortuosity is defined as a pure geometric quantity as, that is, the ratio of path length to the bed thickness, a tortuosity may be defined for each and every channel L_i/L_0, resulting in multiple tortuosities. We shall call this definition of tortuosity the microscopic geometric tortuosity. Alternatively, we define a single "imaginary" (equivalent) channel that has the same "conducting capacity" as the sum of all microscopic channels (Fig. 1), and we then determine the tortuosity as the ratio of length of the equivalent channel to the bed thickness L_{e}/L_0. We shall call this definition the overall (equivalent) hydraulic tortuosity. This hydraulic tortuosity is difficult to be calculated mathematically or measured directly, because the effective length L_{e} of the flow path is not a measurable quantity (Al-Tarawneh et al. 2009). This hydraulic tortuosity may be determined experimentally from either the electrical conductivity measurements or from the diffusion measurements (Al-Tarawneh et al. 2009).

It should be noticed that there are two definitions of tortuosity commonly used in the literature by researchers, as discussed in the book of Bear (1988), specifically, L_{e}/L_0 and $(L_{\mathrm{e}}/L_0)^2$, or $(L/L_{\mathrm{e}})^2$. If tortuosity is treated as a pure geometric variable to define the difference between the length of flow path and the bed depth, L_{e}/L_0 is appropriate. However, if the flow velocity is also considered and L_0/L_{e} is used as the average cosine between the equivalent flow path and the bulk flow direction, then $(L_0/L_{\mathrm{e}})^2$ should be used to account for both flow path length (or hydraulic gradient, as in Bear's book) and the velocity. Since this study deals with the geometric length of flow path, the simple definition of L_{e}/L_0 was adopted.

The tortuosity that is commonly referred to in the literature is the overall (equivalent) hydraulic tortuosity L_{e}/L_0, or $(L_{\mathrm{e}}/L_0)^2$. This tortuosity is often used as an adjustable

parameter and reflects the efficiency of percolation paths, which is linked to the topology of the material, but not reducible to classical measured microstructural parameters like specific surface area, porosity, or pore size distribution (Barrande et al. 2007). To truly understand the flow through a porous medium, it is necessary to understand the pore structures (microstructures) first, and then the flow regimes within the pore structures. The studies of pore structures in the context of tortuosity are very limited in the literature. Some geometric models have been developed for idealized (very simplified) pore structures. For example, Yu and Li (2004) used a two-dimensional (2D) square particle system to represent the porous media in deriving a geometric model for tortuosity. Matyka et al. (2008) studied the tortuosity–porosity relation using a microscopic model of a porous medium arranged as a collection of freely overlapping squares.

Quantifying the microstructure of porous media is extremely difficult. When a porous bed is formed, many factors affect the spacial arrangement of particles (the pore structure). The discrete element method (DEM) which was originally proposed by Cundall (1971) has been shown to be a powerful tool for analysis of granular media (e.g. Ghaboussi and Barbosa 1990; Tavarez and Plesha 2007), and it provides an alternative way to quantify the complex pore structures of porous media. Based on the pore structure predicted by the DEM, each and every microscopic channel for airflow can be quantified in terms of channel length, shape and etc. The objective of this research was to use a discrete element model to qualify the pore structures of bulk grain in three dimensions, from which tortuosity for airflow through the porous bed was determined. As discussed earlier, there are several different definitions of tortuosity. This article focuses on the geometric tortuosity at the microscopic level, defined as L_i/L_0, where L_i is the path length of an individual flow channel and L_0 is the distance between two parallel planes (Fig. 1). The significance of the microscopic geometric tortuosity is that it is determined from the measurable microstructural parameters that dictate the spatial structure of the porous bed.

While theoretically all microscopic flow channels may be quantified once the spatial structure of the bed is created by the DEM, we focused on only the shortest channel as the first step to confirm the suitability of the DEM in quantifying flow channels in porous media. The tortuosity in this article is defined as the minimum geometric tortuosity, determined by Eq. 6 for $L_e = \min(L_i), i = 1, 2, 3$. It should be noted that this definition differs from and is lower than those commonly used in the literature. The future research should explore all microscopic channels, not only the length but also other geometric properties, such as shape, and establish quantitative relationships between the microscopic geometric tortuosities and the flow of fluids in porous beds.

2 Methodology

2.1 Discrete Element Simulation of Spacial Arrangement of Particles in Porous Beds

The flow paths in a porous bed are dictated by the pore structure (microstructure) of the bed. Quantifying the pore structure of real porous beds is still an actively pursued research subject. A discrete element software package (PFC^{3D}) was used to construct models for predicting the pore structure (spacial arrangement of particles) in porous beds (Itasca Consulting Group Inc., Minneapolis, MN). The PFC^{3D} model simulates the movement of every particle in a porous bed during the bed formation processes, such as filling a storage container (bin) with granules. The model calculates interaction forces between adjacent particles, particles and the walls of the containing structure, as well as the gravity and other body forces, and keeps

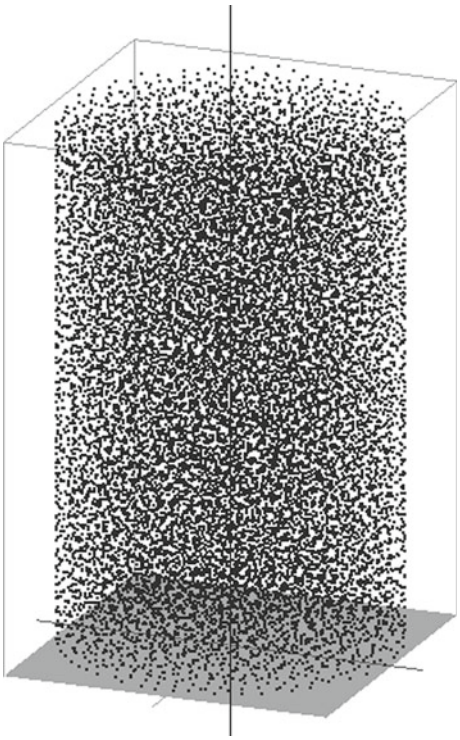

Fig. 2 Visualization of test porous bed

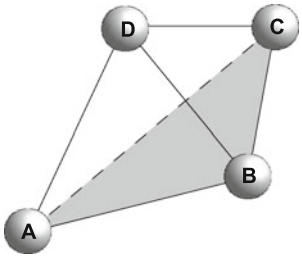

Fig. 3 Illustration of a tetrahedron unit and the base triangle for flow path determination

track of the ongoing relationships between objects. When all particles in the porous bed reach the steady state (equilibrium), the coordinates of all the particles can be obtained.

Simulations were conducted for soybeans in a cylindrical container (bin) of 0.28 m (height) by 0.15 m (diameter) (Fig. 2). The PFC^{3D} model generated 18188 spherical particles of 5.5- to 7.5-mm diameter in the bin, which was filled to a depth of 0.258 m. Details of the simulations, as well as its validation, may be found in the studies of Liu et al. (2008a,b). The simulation results, including the particle identification numbers and coordinates of all particles were obtained from the PFC^{3D} simulations and used in this study.

2.2 Algorithm for Calculating Tortuosity

Airflow paths (channels) in porous beds are connected pores between particles. A tetrahedron consisting of four particles is used as the base unit to determine the airflow path (Fig. 3). Air

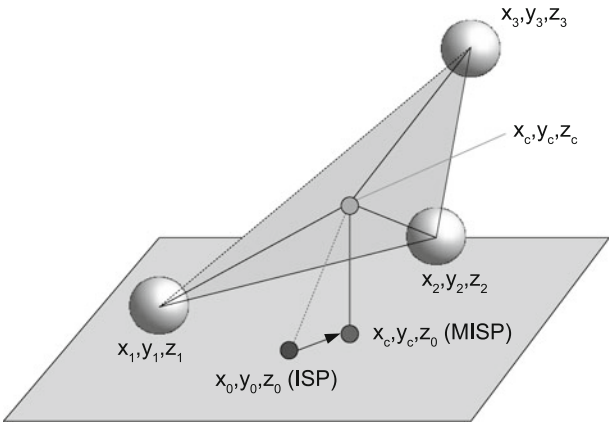

Fig. 4 Illustration of the method of calculating the path length (the particles are not in the scale)

enters the flow channel through the space between particles A, B and C ($\triangle ABC$ is termed the base triangle), and there are three possible paths form air to flow through the tetrahedron unit, that is, through the space between particles A, B and D (represented by $\triangle ABD$), between particles A, C and D ($\triangle ACD$), or between particles B, C and D ($\triangle BCD$). In this study, it is proposed that the shortest path is used to calculate the tortuosity. For example, if the centroid of $\triangle ACD$ is above the other two triangles ($\triangle ABD$ and $\triangle BCD$), the distance connecting the centroids of $\triangle ABC$ and $\triangle ACD$ is used as the length of flow path for calculating the tortuosity because it represents the shortest distance to the top surface of the porous bed.

An algorithm was developed to search through the porous bed particle by particle based on the spacial arrangement of particles simulated by the PFC^{3D} model for the shortest flow path. When air flows from the bottom to the top of a porous bed, many flow paths exist, and each flow path starts at a different location. An initial starting point (ISP) was randomly selected as the air entrance point at the bed bottom. It should be noted that this point should not be close to the vertical walls of the bin to avoid the wall effect on the flow path. Figure 4 illustrates an ISP defined by coordinates (x_0, y_0, z_0).

Once an ISP is selected, the next step is to find three particles nearest to the ISP to form the base triangle of a tetrahedron unit by calculating distances of all surrounding particles to the ISP. When the three particles are selected, the centroid of the triangle formed by the three particles is located as follows (Fig. 4).

$$\begin{aligned} x_c &= \frac{x_1+x_2+x_3}{3} \\ y_c &= \frac{y_1+y_2+y_3}{3} \\ z_c &= \frac{z_1+z_2+z_3}{3} \end{aligned}, \tag{7}$$

where x_c, y_c and z_c are the coordinates of the centroid of the triangle, and x_1, y_1, z_1, x_2, y_2, z_2, x_3, y_3 and z_3 are the coordinates of three particles that form the vertices of the triangle.

Air is assumed to enter the porous bed vertically, but the path from the randomly selected ISP to the centroid of the triangle may not be in the vertical direction (Fig. 4). Therefore, a second point with coordinates (x_c, y_c, z_0) is adopted as the modified ISP (MISP) (Fig. 4), which aligns vertically with the centroid of the triangle and is used as the start point to calculate the path length. A similar process is performed to achieve a vertical flow exist at the top surface of the bed.

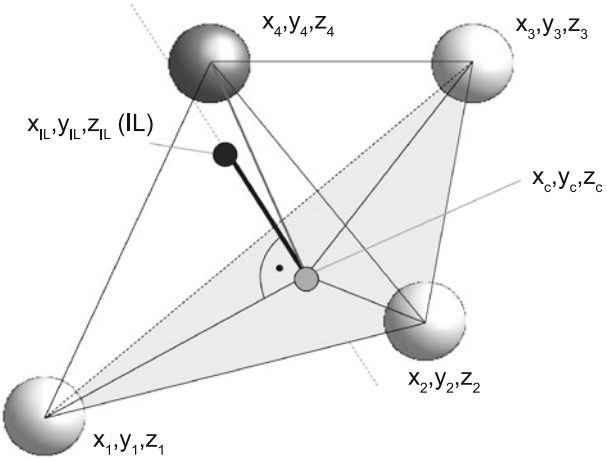

Fig. 5 Method of determining the top corner of the tetrahedron

To define the physical depth of the porous bed, the data from the PFC^{3D} simulations are sorted by the z coordinate. The particle with the lowest value of z coordinate (z_1) is used to define the bottom layer of the bed, and the particle with the highest value of z coordinate (z_{n_s}) is used to define the upper surface of the porous bed. The depth of porous bed L_0 (m) is then calculated as follows:

$$L_0 = (z_{n_s} - z_1) + d_{\text{ave}}, \tag{8}$$

where z_{n_s}—coordinate of the highest sphere in the porous bed (m), z_1—coordinate of the lowest sphere in the porous bed (m) and d_{ave}—average particle diameter (m).

After the base triangle is established, the next step is to find a particle as the fourth vertex to construct a tetrahedron. That is, three vertices of the tetrahedron are defined by the known coordinates of the base triangle (x_1, y_1, z_1), (x_2, y_2, z_2) and (x_3, y_3, z_3), the fourth particle (x_4, y_4, z_4) is to be selected. There are many particles surrounding the three particles forming the base triangle, therefore, more than one particle could be selected as the fourth particle of the tetrahedron unit. Since the goal is to find the closest particle, hexagonal close-packing which has the maximum possible density for both regular and irregular arrangements of equal spheres in the porous bed (Kepler conjecture) is first considered to find the ideal location (IL) for the fourth particle. In other words, it is attempted to find a fourth particle to form a regular tetrahedron with the base triangle.

To establish the ideal location (x_{IL}, y_{IL}, z_{IL}) (Fig. 5), the normal direction of the base triangle is determined by using the cross product of two vectors $\overrightarrow{w}$ and $\overrightarrow{u}$ representing the directions of sides 1–2 and 1–3 of the triangle:

$$\begin{aligned} w_x &= x_2 - x_1 \qquad u_x = x_3 - x_1 \\ w_y &= y_2 - y_1 \qquad u_y = y_3 - y_1 \\ w_z &= z_2 - z_1 \qquad u_z = z_3 - z_1 \end{aligned}. \tag{9}$$

The components of the vector presenting the normal direction of the base triangle are obtained as follows:

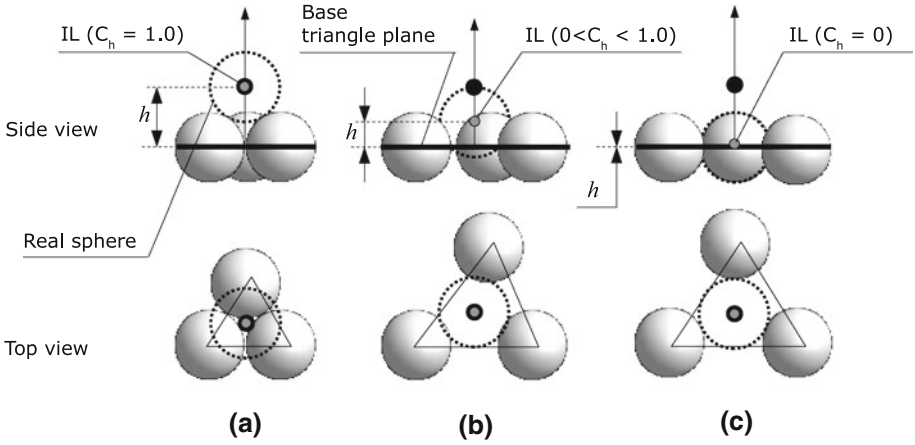

Fig. 6 Illustration of ideal height of tetrahedron

$$\begin{aligned} \alpha &= w_y \cdot u_z - u_y \cdot w_z \\ \beta &= u_x \cdot w_z - w_x \cdot u_z \\ \gamma &= w_x \cdot u_y - u_x \cdot w_y \end{aligned} . \tag{10}$$

The vector is then normalized

$$\alpha = \frac{\alpha}{\delta}, \beta = \frac{\beta}{\delta}, \gamma = \frac{\gamma}{\delta}, \tag{11}$$

where δ is the length of the vector presenting the normal direction of the base triangle and determined as follows:

$$\delta = \sqrt{\alpha^2 + \beta^2 + \gamma^2}. \tag{12}$$

It should be noted that mathematically there are two opposite normal directions for the base triangle, depending on the sequence of selecting points calculating vectors $\overrightarrow{w}$ and $\overrightarrow{u}$. Since air flows upwards, the normal direction in the upward direction should be used. If the calculated normal vector is in the downward direction, a different sequence will be used to select the points to re-calculate vectors $\overrightarrow{w}$ and $\overrightarrow{u}$ until an upward normal vector is obtained.

In the ideal hexagonal close-packing, the distance between the fourth particle and the plane of the base triangle is $l_{\text{ave}} \cdot \sqrt{2/3}$, where l_{ave} is the average length of side in base triangle (m). Given that particle packing in porous beds is generally not regular, a correction coefficient C_{h} is introduced to calculate the distance of the IL to the plane of the base triangle

$$h = C_{\text{h}} \cdot l_{\text{ave}} \cdot \sqrt{\frac{2}{3}}, \tag{13}$$

where h is the tetrahedron height (m), C_{h} is the height correction coefficient (–) ($0 < C_{\text{h}} \leq 1$). Now, the coordinates of the IL can calculated as follows:

$$\begin{aligned} x_{\text{IL}} &= x_{\text{c}} + \alpha \cdot C_{\text{h}} \cdot l_{\text{ave}} \cdot \sqrt{\tfrac{2}{3}} \\ y_{\text{IL}} &= y_{\text{c}} + \beta \cdot C_{\text{h}} \cdot l_{\text{ave}} \cdot \sqrt{\tfrac{2}{3}} \\ z_{\text{IL}} &= z_{\text{c}} + \gamma \cdot C_{\text{h}} \cdot l_{\text{ave}} \cdot \sqrt{\tfrac{2}{3}} \end{aligned} . \tag{14}$$

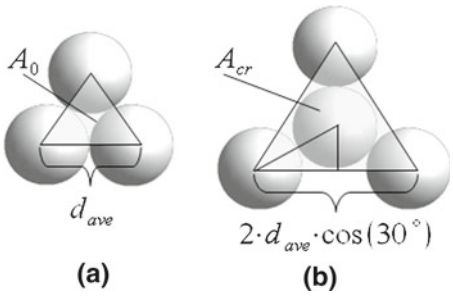

Fig. 7 Illustration to the critical triangle aspect

The scenario of $C_h = 1$ corresponds to the hexagonal close-packing the formed tetrahedron is regular, with lengths of sides l_{ave} equal to d_{ave} (Fig. 6a). However, the actual packing in porous beds is generally less dense than the hexagonal close-packing. Therefore, more space may exist between the three particles forming the base triangle to allow the fourth particle to be closer to the triangle basis, i.e. $C_h < 1$ (Fig. 6b). This issue is discussed further in Sect. 3.

It should be noted that there may not be a particle existing exactly at the ideal location in the porous bed. The particle that is closest to the IL will then be selected as the fourth point to establish the tetrahedron unit (Fig. 5). The quality of location prediction (closeness) is measured by a dimensionless indicator I_F (closeness index) defined as follows:

$$I_F = \frac{\sqrt{(x_{IL} - x_4)^2 + (y_{IL} - y_4)^2 + (z_{IL} - z_4)^2}}{0.5 \cdot d_{ave}}. \tag{15}$$

I_F measures the closeness of the selected fourth particle to the IL, relative to the particle size. For $I_F < 1$, the fourth particle is within the average radius of particle, and in other words the IL is situated inside the fourth particle; $I_F = 1$ means that the IL is exactly on the surface of the fourth particle; and $I_F > 1$ indicates that the fourth particle is located at a distance greater than the average particle radius. As I_F increases, the shape of the tetrahedron deviated further from a regular tetrahedron, and predicted location of the fourth sphere becomes less suitable for constructing the tetrahedron.

The established tetrahedron has the base triangle, plus three new face triangles (Fig. 5). It has to be decided which of these three new triangles will be used as the base triangle for the next tetrahedron. As discussed earlier, the shortest airflow path to the upper surface is used in calculating the tortuosity. Therefore, the two of the new triangles associated with the lowest point of tetrahedron (the farthest distance to the upper surface) are not considered, and the remaining new triangle is used as the base to establish the next tetrahedron. In other words, the segment of flow path within the current tetrahedron unit follows the line that connects the centroids of the base triangle and the new triangle at the highest location. Before proceeding to establishing the next tetrahedron (flow segment), the area of the base triangle (A_i) is checked for compatibility. Specifically, the area of the base triangle must be greater than that (A_0) of an equilateral triangle formed by three touching particles (Fig. 7a), and smaller than that (A_{cr}) of an equilateral triangle with an inscribed circle of diameter d_{ave} (Fig. 7b). Area A_0 is the smallest triangle that could physically exist, and any triangles with areas greater than A_{cr} would be subjected to re-configuration (unstable) because the void space is large enough to allow another particle to enter the void.

To ensure the condition $A_0 \leq A_i \leq A_{cr}$ is satisfied, an area ratio I_A is calculated as an indicator and checked at each iteration in establishing tetrahedrons.

$$I_A = \frac{A_i}{A_0}. \tag{16}$$

The area of the base triangle is calculated by the Huron equation (Bronsztejn and Siemiendiajew 1988)

$$A_i = \sqrt{\frac{L}{2} \cdot \left(\frac{L}{2} - a\right) \cdot \left(\frac{L}{2} - b\right) \cdot \left(\frac{L}{2} - c\right)}, \tag{17}$$

where L is the triangle circumference (m), and a, b and c are the length of three sides of triangle, respectively. The areas of the smallest (A_0) and largest (A_{cr}) equilateral triangles are calculated as follows:

$$A_0 = \frac{1}{2} \cdot d_{ave} \cdot \frac{\sqrt{3}}{2} \cdot d_{ave} = \frac{\sqrt{3}}{4} \cdot d_{ave}^2, \tag{18}$$

$$A_{cr} = \frac{1}{2} \cdot 2 \cdot d_{ave} \cdot \cos(30) \cdot \frac{\sqrt{3}}{2} \cdot 2 \cdot d_{ave} \cdot \cos(30) = 3 \cdot \frac{\sqrt{3}}{4} \cdot d_{ave}^2. \tag{19}$$

The upper bound of the area ratio is reached when A_i reaches A_{cr}, and this upper bound is termed the critical triangle area indicator and calculated as follow:

$$I_A^{cr} = \frac{3 \cdot \frac{\sqrt{3}}{4} \cdot d_{ave}^2}{\frac{\sqrt{3}}{4} \cdot d_{ave}^2} = 3. \tag{20}$$

The criterion $A_0 \leq A_i \leq A_{cr}$ can now be rewritten as:

$$1 \leq I_A \leq 3. \tag{21}$$

At first step, if the value of the index I_A is greater than or equal to I_A^{cr}, a new search of the nearest three spheres to the current triangle centre is begun. After this correction, the all next steps of the algorithm must be repeated.

Once the tetrahedron is established and the base triangle is selected for the next iteration (tetrahedron), the process is repeated until the upper surface of the porous bed is reached. The total path length is then calculated as the sum of distances connecting the centroids of base triangles at each iteration, and the tortuosity is determined as the ratio between the total flow path length to the depth of porous bed.

3 Results and Discussion

3.1 Determining Height Correction Coefficient C_h

The algorithm described in Sect. 2.2 requires specifying the optimal value(s) of correction coefficient C_h. Numerical experiments were performed to determine the influence of correction coefficient C_h on the tortuosity. As mentioned earlier, the method developed in this study attempts to find the shortest path length or the lowest tortuosity value. The simulation results showed that the tortuosity varied from 1.20 to 1.30, or 8% when C_h was changed from 0.1 to 1.0. The minimum tortuosity of 1.20 occurred at $C_h = 0.4$ (Fig. 8). For $C_h = 1.0$ the tortuosity was equal to 1.24 (m/m). It is worth noting that the values of C_h in range of 0.40–0.55 resulted in the same number of the path points (flow segments) n_p (Fig. 8). The result

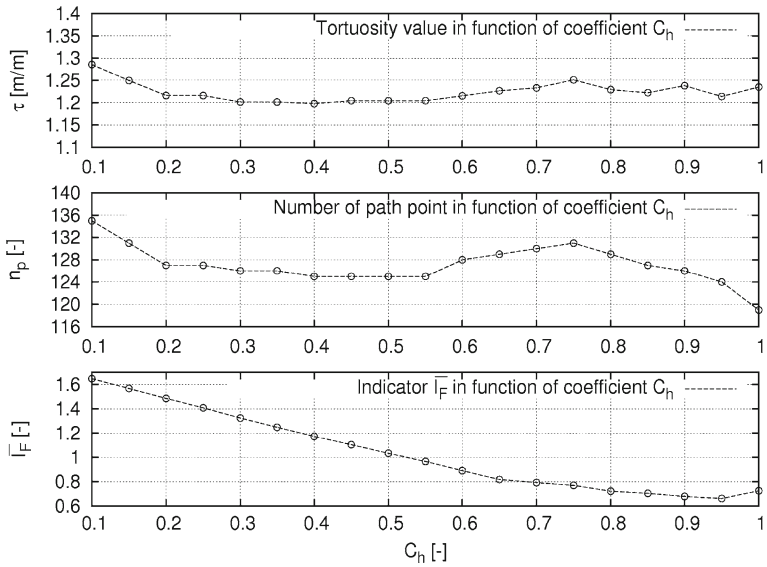

Fig. 8 Influence of coefficient C_h on the calculation results

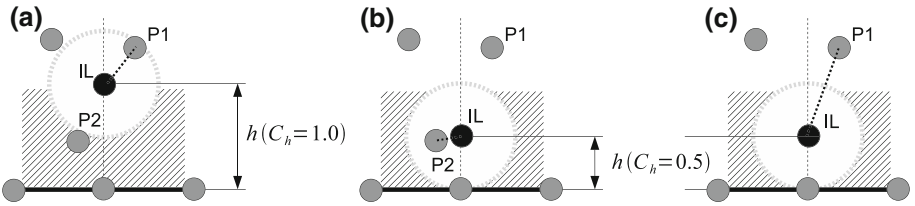

Fig. 9 Schematic explanation of the optimal value of the coefficient C_h

indicates that the model sensitivity to the value of C_h around the optimal point (0.30–0.55) is negligible.

It is critical to select a value <1.0 for the correction coefficient C_h, as explained schematically in Fig. 9. For $C_h = 1.0$, the ideal location (IL) is relatively high and it can happen that the closest particle to the IL may be a particle (P1) above this point (Fig. 9a), while another particle which is closer to the base triangle plane (P2) is missed. In the scenarios illustrated, particle P2 should be used as the fourth particle to establish the tetrahedron unit because of its closeness to the base triangle plane. In other words, reducing the C_h value increases the probability of locating the fourth particle to form a stable tetrahedron (Fig. 9b).

As the correction coefficient C_h decreases, the closeness index I_F increases (worsens), particularly I_F becomes >1.0 when C_h is <0.5 (Fig. 8). This is explained by Fig. 9. The introduction of C_h reduces the distance between the IL and the triangle base in each tetrahedron, whether there exists a P2 particle (Fig. 9b) or not (Fig. 9c). If a P2 particle exists then smaller value of C_h helps to "catch" it (Fig. 9b), and the value of I_F would be very small (good). However, if the closest particle is P1 (i.e. P2 does not exist) (Fig. 9c), the distance between P1 and IL would be bigger, which would result in a large value of I_F. The numerical simulations have indicated that the majority of tetrahedron units are formed without the existence of P2

particles (Fig. 9c). Therefore, the average value of I_F from all iteration cycles increases with decreasing C_h value.

The goal of this algorithm is to calculate the lowest value of tortuosity among all possible flow paths. Although the minimum tortuosity of occurred at $C_h = 0.4$ (Fig. 8), the difference in tortuosity value for C_h values in the range from 0.4 to 0.5 is practically negligible (0.5%). However, the I_F value decreases about 12% when C_h changed from 0.4 to 0.5. This indicates that the optimal value of C_h is 0.5.

3.2 Variable Height Correction Coefficient

As indicated in Fig. 6, the height correction coefficient C_h varies with the void space between three particles forming the base triangle, or with the area of the base triangle. Specifically, $C_h = 1.0$ if $I_A = (A_i/A_0) = 1$ (Fig. 6a), and $C_h \mapsto 0$ as $I_A \mapsto I_A^{cr}$ (Fig. 6c). Therefore, in principle, a constant value should not be assigned to C_h, and C_h should be expressed as a function of I_A. Therefore, Eq. 13 is modified as follows:

$$h = C_h^f\,(I_A) \cdot \sqrt{\frac{2}{3}} \cdot l_{ave}. \tag{22}$$

The function for $C_h^f\,(I_A)$ should be asymmetric, and allow for a smooth and reconfigurable transition between the two values (0 and 1). An exponential function meets this requirement (Sobieski 2009):

$$C_h^f\,(I_A) = 1 - \frac{\exp\left(a \cdot (I_A - b)\right)}{1 + \exp\left(a \cdot (I_A - b)\right)}. \tag{23}$$

The function for C_h is designed to achieve the following:

$$\begin{cases} C_h^f\,(I_A = 1) = 1 \\ C_h^f\left(I_A = \bar{I_A}\right) = 0.5 \\ C_h^f\left(I_A = I_A^{cr}\right) = 0 \end{cases}, \tag{24}$$

where $\bar{I_A}$ is the average value of I_A for all tetrahedron units in the porous bed. The empirical coefficient a in the function is responsible for the rate of change in function value. As the value of this coefficient increases, the function decreases more rapidly with I_A (Fig. 10). For $a = 0$, the function $C_h\,(I_A)$ becomes a constant of 0.5, which is the optimal value of C_h (if C_h is treated as a constant). The value of coefficient a can be determined using the criterion of achieving the smallest tortuosity. The coefficient b should be equal to the average value of I_A. For the porous bed simulated in this study, it was found that $\bar{I_A} \approx 1.3$.

A series of simulations were conducted to test the model sensitivity to the coefficient a. It was observed that the model was not sensitive to the coefficient value in a certain range. Specifically, for a values between 2.5 and 9.0, the total number of path points (segments) n_p remained unchanged, and the tortuosity τ was also practically the same (Fig. 11). It is worth noting that the value of the closeness index I_F stayed below 1, indicating that the fourth particle selected for constructing each tetrahedron was in the close vicinity of the base triangle and tetrahedrons were structurally stable. The tortuosity, number of path points, and the distance ratio $\bar{I_F}$ all started to increase after the a coefficient reached 9. To not use the value from the end of the range, a value of 8 will be used in the following discussion. In this way the authors want to avoid a situation in which a small factor

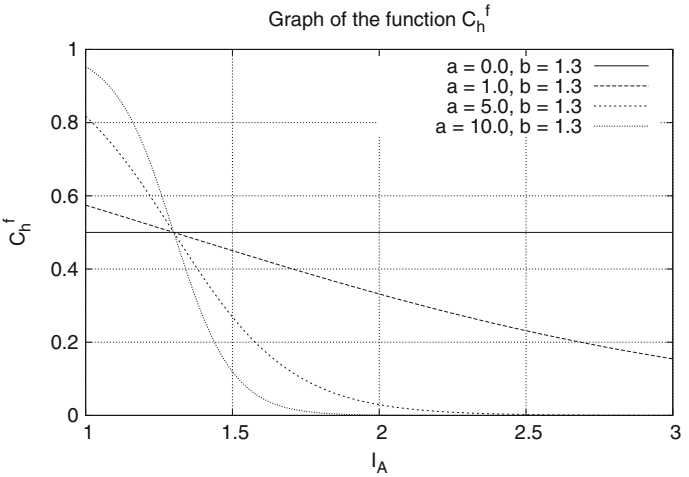

Fig. 10 Value of the function C_h depending on the a coefficient

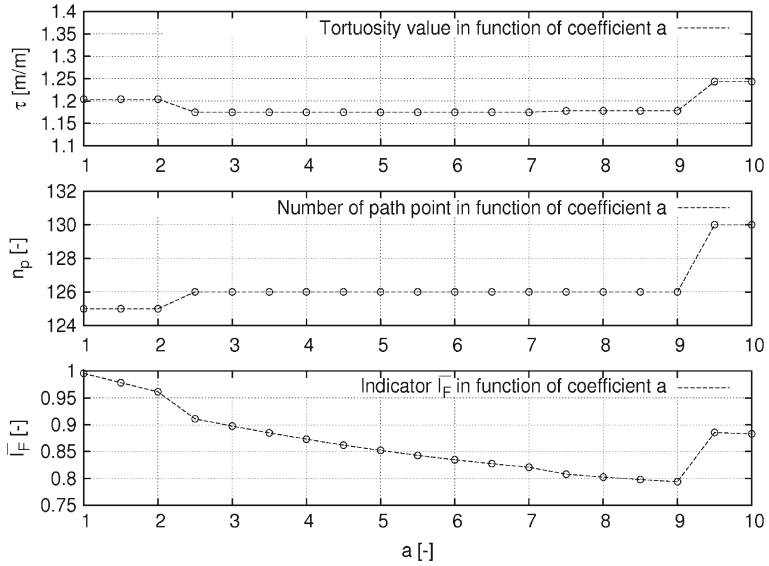

Fig. 11 Influence of coefficient a on the calculation results

causes a sudden increase in tortuosity. Using, $C_\mathrm{h}^f(a = 8.0, b = 1.3)$, the calculated tortuosity was 1.18, which was lower than that (1.20) obtained for constant C_h in the range of 0.30–0.55. Also, the average closeness index $\bar{I}_\mathrm{F}$ was 0.8, which is lower (better) than the scenarios of using a constant C_h of 0.5. Interestingly, the number of path points ($n_\mathrm{p} = 126$) is almost the same as that (125) for the constant C_h. However, the difference in tortuosity between the two approaches indicates that these pass points are not the same points in the two approaches.

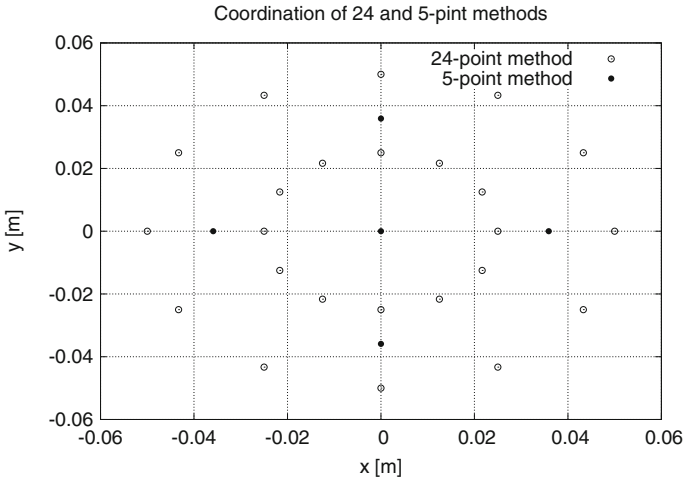

Fig. 12 Locations of ISP in 24- and 5-point simulations

3.3 Flow Paths for Different Starting Points

The model generates different flow paths if different ISP are selected. So far, discussion has been focused on the start point located centrally (so called 1-point method). In this section, flow paths generated from different start points are compared. The authors propose two basic methods, one with 24 ISP's and the other one with 5 IPS's. Coordinates of ISP in *XY* plane are shown in Fig. 12. All calculations in this section were based on the parameters described in Sect. 3.2.

The average tortuosity value obtained by using 24-point method was 1.2172, with the minimum and maximum values of 1.1590 and 1.2575, repetitively. The total numbers of path segments (n_p) ranged from 119 to 131. In the 5-point method, the average value of tortuosity was 1.2219, with the minimum 1.1780 and the maximum 1.2747. The n_p value was between 126 and 133. In next stage of investigations an other set of calculation were performed, this time with 100 different ISP's (other than that in previous methods). The average tortuosity for this case was 1.2167, and the minimum and the maximum value were equal to 1.1431 and 1.2921, repetitively. The relative errors between 100 ISP method and 24 and 5 ISP are equal to 0.0385 and 0.4248%, repetitively. Based on these results, it was assumed that the 5 ISP method should be sufficient in calculating the tortuosity. The results for the 5-point calculation are collected in Table 1 and the corresponding flow paths are shown in Fig. 13. The relative error is calculated from the formula:

$$\delta = \left| \frac{\tau_i - \tau_\mathrm{ave}}{\tau_\mathrm{ave}} \right| \cdot 100\%, \tag{25}$$

where τ_i is the tortuosity calculated for ith point and τ_ave is the average value of tortuosity calculated for all points.

3.4 Path Smoothing

Construction of flow paths in this study is purely based on geometrical relations among tetrahedrons that geometrically represent particles and pores in a porous bed. It is noticed that

Table 1 Calculated tortuosity by using five ISP

ISP	x (m)	y (m)	τ (m/m)	n_p (–)	δ (%)
1	0.0	0.0	1.1780	126	3.59
2	0.0359	0.0	1.2284	129	0.53
3	−0.0359	0.0	1.2442	133	1.82
4	0.0	0.0359	1.1843	126	3.08
5	0.0	−0.0359	1.2747	132	4.32
Average			1.2219	129.2	2.67

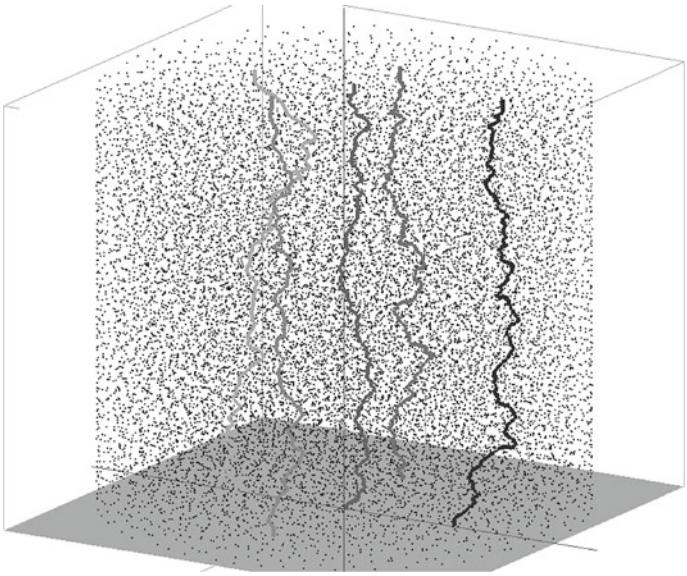

Fig. 13 Paths for different start points

connecting tetrahedron units to form a flow path results in some sharp angles in the flow path (Fig. 14). It is known that a fluid can not flow in such a way. Therefore, a method is proposed to "smooth" the sharp turns.

The path smoothness is carried out locally, i.e. each connection point between two flow segments (tetrahedron units) is examined first by calculating the turn angle ω_i between the two adjacent segments as follows (Fig. 15a):

$$\omega_i = \frac{a_i^2 + b_i^2 - c_i^2}{2 \cdot a_i \cdot b_i}, \tag{26}$$

where the index $i = 1$ to n_p, representing the number of the current path point. Variables a_i, b_i and c_i are lengths of the sides of the triangle formed by three neighboring path points, respectively (Fig. 15a). Using the data obtained in Sect. 3.2, the turn angle was calculated to be 139° on average and the results are shown in Fig. 16.

Lets consider the path length connecting the mid points of two adjacent flow segments and this length is $(\frac{a_i}{2} + \frac{b_i}{2})$ (thick lines in Fig. 15b). If a sharp turn is smoothed by using an arc (thick line in Fig. 15c), the length of this turn would be reduced by a factor ω_i^{cor}. This

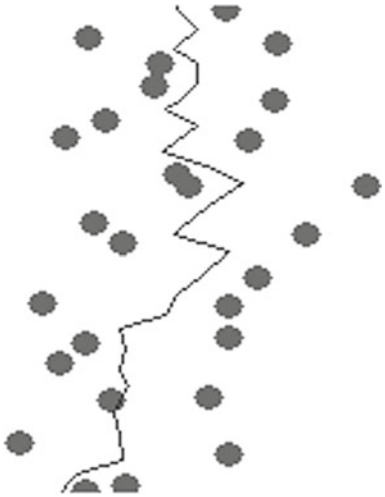

Fig. 14 A fragment of path with sharp shapes

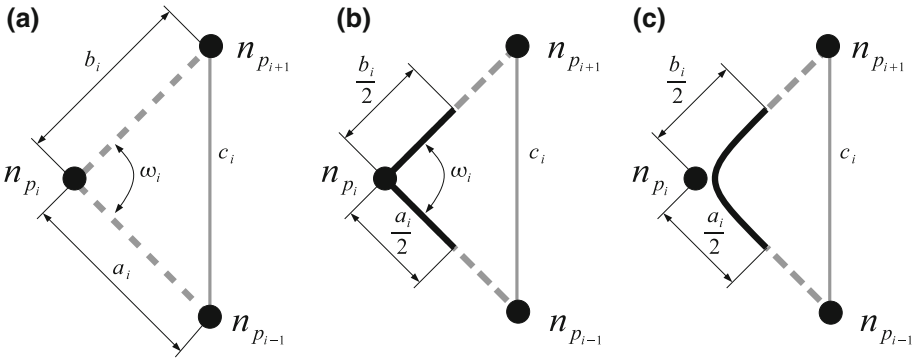

Fig. 15 Schematic representation of the method of smoothing the path (need to **a**, **b** and **c**)

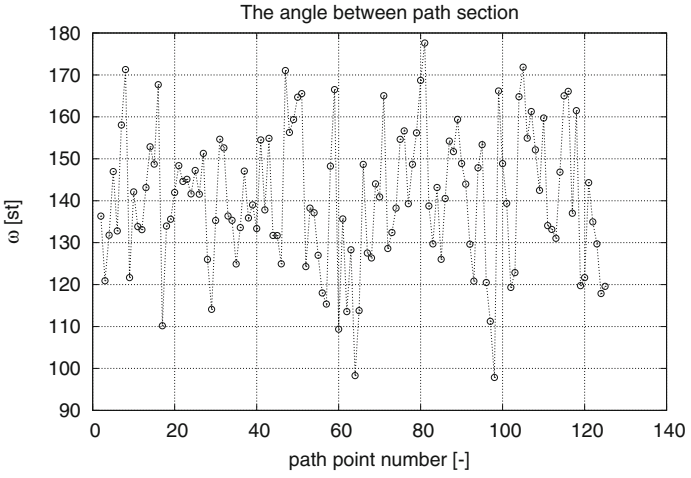

Fig. 16 The values of the angles between the various path segments for the "final case"

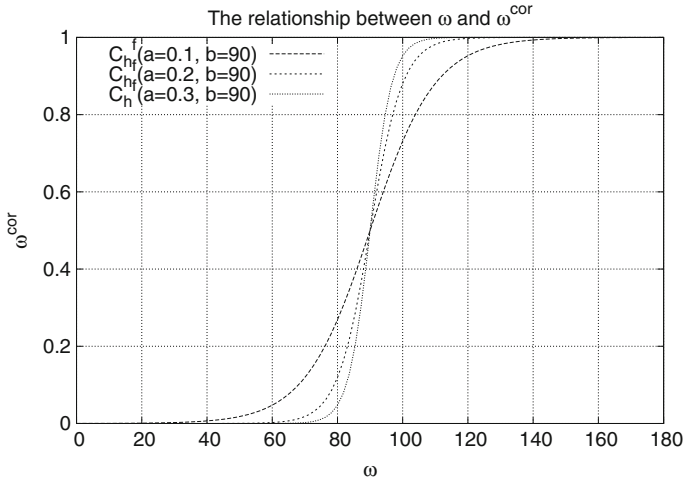

Fig. 17 Relationship between ω and ω^{cor}

reduction factor ω_i^{cor} varies with the turn angle ω_i. Theoretically, the reduction factor ω_i^{cor} should be 1 for $\omega_i = 180$ (no reduction required) and 0 for $\omega_i = 0$ (this is prevented in the algorithm when selecting tetrahedron units for constructing the flow path, also see Fig. 16). The following function is proposed for ω_i^{cor} to meet the theoretical requirements:

$$\omega_i^{\text{cor}} = \frac{\exp\left(\omega_a \cdot (\omega_i - \omega_b)\right)}{1 + \exp\left(\omega_a \cdot (\omega_i - \omega_b)\right)}, \tag{27}$$

where ω_a is an empirical constant that is selected to control the rate of change in coefficient ω_i^{cor}, and ω_b is equal to 90°. Equation 26 is graphically presented in Fig. 17. The value of ω_i^{cor} approaches 1 for $\omega_i = 180$, and 0 for $\omega_i = 0$. After applying the correction, the formula for the length of the path will have the form of:

$$L_{\text{e}}^{\text{cor}} = \frac{1}{2} \cdot \left(a_1 + b_{n_{\text{p}}}\right) + \sum_{2}^{n_{\text{p}}-1} \frac{1}{2} \cdot (a_i + b_i) \cdot \omega_i^{\text{cor}}. \tag{28}$$

The first term in the equation takes into account the first half of the first segment (bottom of bed) and the last half of last segment of the path. Under the summation sign is the sum of the halves of sections adjacent to the current path point multiplied by the value of the correction coefficient ω_i^{cor}.

The criteria for selecting optimal ω_a values has yet to be established. Figure 18 shows the effect of coefficient ω_a on the calculated value of tortuosity using parameters in Sect. 3.2 and the 5-point method. The tortuosity increases from 1.0946 to 1.1851 when ω_a varied from 0.05 to 0.1. Although it is known that air flow does follow sharp corners, and thus the actual path would be shorter than that calculated with sharp turns (un-smoothed), it is not known how much shorter without knowing the actual flow properties (velocity, viscosity, surface friction, etc.). Therefore, the required degree of smoothing will depend on the properties of porous bed and flow behaviour. It is suggested that the coefficient ω_a be treated as a constant in the model which is to be calibrated for each porous bed.

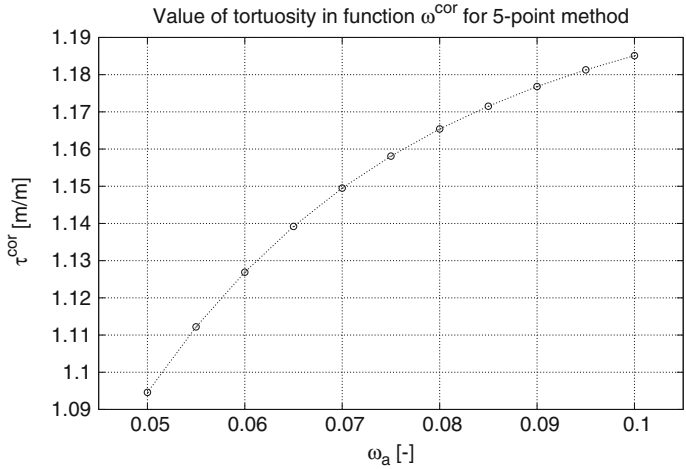

Fig. 18 Influence of coefficient ω_a on the value of tortuosity for the 5-point method

3.5 Comparison with Experiment Data

Little information is available in the literature on tortuosity values because of great difficulties associated with measuring the tortuosity. However, most of porous beds consisting of spherical or quasi-spherical particles have a tortuosity in the range 1–1.4 (Barrande et al. 2007; Dias et al. 2006; Koponen et al. 1996, 1997; Mota et al. 1999; Perret et al. 1999; Yun et al. 2005). An article published by Neethirajan et al. (2006) used the CT imaging technique to quantify the structure of porous beds consisting of cereal grains. They studied three types of grain: wheat, barley and peas. Since peas have similar shape and size to soybeans used in this study, the results for peas are compared with model simulations. The average diameter of peas reported by Neethirajan et al. was 7.27 mm, which is in the range of particle sizes simulated in this study (5.5–7.5 mm). The shapes of soybean and pea kernels used in this study were very similar in terms of sphericity. The average length (a), width (b), and thickness (c) of soybean kernels were measured to be 7.6, 6.7 and 5.7 mm, respectively. The corresponding values for the peas used in the CT experiments were: $a = 7.9$, $b = 7.2$ and $c = 6.7\,(mm)$ (Neethirajan et al. 2006). The average equivalent diameter was 6.7 mm for soybeans which is 9% smaller than that for peas (7.2 mm). The sphericity was calculated to be 0.988 for soybeans and 0.995 for peas, using the equation by Jain and Bal (1997).

The three locations were randomly selected from a CT image to visually construct flow paths by connecting the closest pores to establish the shortest flow path. The lengths of these three paths were then estimated to be 133.88, 136.55 and 136.51, respectively (Fig 19, the unit is not needed here for calculating the tortuosity). The bed height was 128.19, and thus the three corresponding tortuosity values were 1.08, 1.06 and 1.07. These tortuosity values are based on paths constructed from a 2D image (XZ plane), and not the true tortuosity in three dimensions. However, these values indicate that the flow path in the XZ plane is 8.34, 6.52 and 6.49% longer than the bed depth at three locations, respectively. Assuming that similar ratios exist in the YZ plane, the path length in three dimensions may be estimated as $2 \times 8.34\%$, $2 \times 6.52\%$ and $2 \times 6.49\%$ longer than the bed depth. Under this assumption, the value of tortuosity would be 1.1668, 1.1304 and 1.1298, for the three locations, respectively, and an average value of 1.1423.

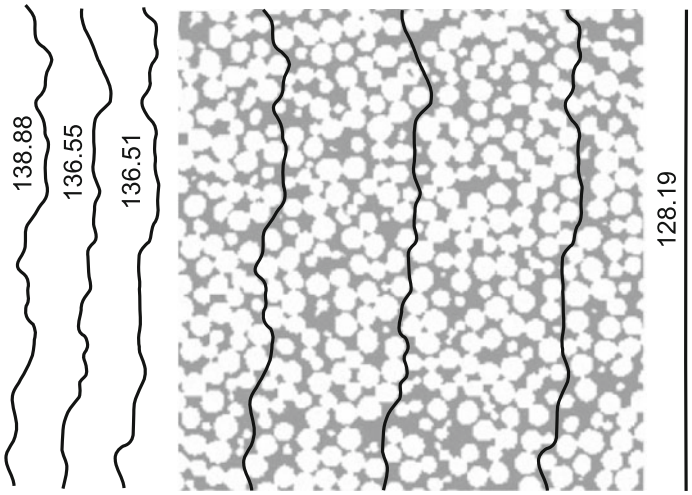

Fig. 19 Sample paths for the peas bed outlined in the study

Table 2 Comparison on results obtained with different approaches

LP	Method	ω_a (m)	τ (m/m)	δ (%)
1	1-Point method without smoothing	–	1.1780	3.13
2	1-Point method with smoothing	0.0866	1.1423	0.00
3	5-Point method without smoothing	–	1.2219	6.97
4	5-Point method with smoothing	0.0665	1.1425	0.02

Table 2 shows comparisons of four scenarios of model prediction with the measured tortuosity value. With smoothing, the model predicts tortuosity values which are almost identical to the measured value for using both 1 and 5 ISP if proper values of ω_a is selected. The predicted tortuosity values are in good agreement with the measured value without smoothing (the relative difference is <7%).

4 Conclusions

This research shows that the discrete element method may provide a new revenue to calculate the tortuosity in porous beds. The discrete element method can simulate the spacial arrangement of particles in porous beds, based on which local (geometrical) flow paths can be constructed. The constructed flow paths truly reflect the pore structures in the porous beds. The close agreement between the tortuosity values predicted by this method and the values obtained from a CT image published in the literature provides substantial confirmation for both the physical basis and the numerical algorithm described in this article.

Since the flow paths are determined purely from the geometric relationships between particles in the porous bed, some sharp turns appear in the constructed (geometrical) flow paths. Although sharp turns may exist geometrically in the porous beds, flow of fluid cannot make sharp turns. Therefore, the geometrical flow paths would be longer than the actual fluid flow paths. It is possible to smooth sharp turns in the geometrical flow paths using mathematical

or fluid mechanics methods. The mathematical smoothing method developed in this research needs to be calibrated to reflect the sharpness of turn as well as the fluid properties, both affecting how a fluid flows through a sharp turn. This requires further research.

This study was focused on developing a new method for quantifying the geometric length of flow channels at pore scale in bulk grain, and a specially defined tortuosity—the ratio of the shortest flow path to the bed depth was calculated to confirm the suitability of the method. Since the properties of fluid were not are considered, the results are not applicable to other fluids, such as water in soil. However, the approach of using the DEM to predict the pore structures of randomly packed particles in three dimensions, based on which the microscopic flow channels are quantified, could be used for other fluid-porous bed systems.

Acknowledgments The financial support for this project is provided by the Natural Science and Engineering Council of Canada.

References

Al-Tarawneh, K.K., Buzzi, O., Krabbenhoft, K., Lyamin, A.V., Sloan, S.W.: An indirect approach for correlation of permeability and diffusion coefficients. Defect Diffus. Forum **283–286**, 504–514 (2009)

Amao, A.M.: Mathematical model for darcy forchheimer flow with applications to well performance analysis. MSc Thesis, Department of Petroleum Engineering, Texas Tech University, Lubbock, TX, USA (2007)

Andrade, J.S., Costa, U.M.S., Almeida, M.P., Makse, H.A., Stanley, H.E.: Inertial effects on fluid flow through disordered porous media. Phys. Rev. Lett. **82**(26), 5249–5252 (1999)

Barrande, M., Bouchet, R., Denoyel, R.: Tortuosity of porous particles. Anal. Chem. **79**(23), 9115–9121 (2007)

Bear, J.: Dynamics of Fluids in Porous Media. Dover Publications, New York (1988)

Bear, J., Bachmat, Y.: Introduction to Modeling of Transport Phenomena in Porous Media. Kluwer, Dordrecht (1991), ISBN 0792305574

Belyadi, A.: Analysis Of single-point test to determine skin factor. PhD Thesis, Department of Petroleum and Natural Gas Engineering, West Virginia University, Morgantown, West Virginia, USA (2006a)

Belyadi, F.: Determining low permeability formation properties from absolute open flow potential. PhD Thesis, Department of Petroleum and Natural Gas Engineering, West Virginia University, Morgantown, West Virginia, USA (2006b)

Bronsztejn, I.N., Siemiendiajew, K.A.: Mathematic (Part I). PWN Scientific Publishing, Warsaw (1988)

Cundall, P.A.: A computer model for simulating progressive, large-scale movements in blocky rock systems. In: Proceedings of International Rock Mechanics Symposium, vol. 2, no. 8, pp. 11–18 (1971)

Dias, R., Teixeira, J.A., Mota, M., Yelshin, A.: Tortuosity variation in a low density binary particulate bed. Sep. Purif. Technol. **51**(2), 180–184 (2006)

Ewing, R., Lazarov, R., Lyons, S.L., Papavassiliou, D.V., Pasciak, J., Qin, G.X.: Numerical well model for non-Darcy flow. Comput. Geosci. **3**(3-4), 185–204 (1999)

Fourie, W., Said, R., Young, P., Barnes, D.L.: The simulation of pore scale fluid flow with real world geometries obtained from X-ray computed tomography. COMSOL Conference, Boston, USA, March 14 (2007)

Ghaboussi, J., Barbosa, R.: Three-dimensional discrete element method for granular materials. Int. J. Numer. Anal. Methods Geomech. **14**, 451–472 (1990)

Hellstrm, J.G.I., Lundstrm, T.S.: Flow through porous media at moderate Reynolds number. In: 4th International Scientific Colloquium: Modelling for Material Processing, University of Latvia, Riga, Latvia, June 8–9 (2006)

Hernndez, R.: Combined flow and heat transfer characterization of open cell aluminum foams. MSc Thesis, Mechanical Engineering, University Of Puerto Rico, Mayagez Campus, San Juan, Puerto Rico (2005)

Jain, R.K., Bal, S.: Properties of pearl millet. J. Agric. Eng. Res. **66**, 85–91 (1997)

Koponen, A., Kataja, M., Timonen, J.: Tortuous flow in porous media. Phys. Rev. E **54**(1), 406–410 (1996)

Koponen, A., Kataja, M., Timonen, J.: Permeability and effective porosity of porous media. Phys. Rev. E **56**(3), 3319–3325 (1997)

Littmann, W.: Gas flow in porous media—turbulence or thermodynamics. Oil Gas Eur. Mag. **30**(Part 4), 166–169 (2004)
Liu, C., Zhang, Q., Chen, Y.: PFC^{3D} Simulations of lateral pressures in model bin. ASABE International Meeting, paper number 083340. Rhode Island, USA (2008a)
Liu, C., Zhang, Q., Chen, Y.: PFC^{3D} Simulations of vibration characteristisc of bulk solids in storage bins. ASABE International Meeting, paper number 083339. Rhode Island, USA (2008b)
Lord, D.L., Rudeen, D.K., Schatz, J.F., Gilkey, A.P., Hansen, C.W.: DRSPALL: spallings model for the waste isolation pilot plant 2004 recertification. SANDIA REPORT SAND2004-0730, Sandia National Laboratories, Albuquerque, New Mexico 87185 and Livermore, CA 94550, February (2006)
Lu, J., Guo, Z., Chai, Z., Shi, B.: Numerical study on the tortuosity of porous media via lattice Boltzmann method. Commun. Comput. Phys. **6**(2), 354–366 (2009)
Matyka, M., Khalili, A., Koza, Z.: Tortuosityporosity relation in the porous media flow. Phys. Rev. E **78**, 026306 (2008)
Mian, M.A.: Petroleum Engineering Handbook for the Practicing Engineer, vol. 2. Pennwell Publishing, Tulsa, Oklahoma, USA (1992)
Mitosek, M.: Fluid Dynamics in Engineering and Environmental Protection. Warsaw University of Technology, Warsaw (2007) (in Polish)
Miwa, S., Revankar, S.T.: Hydrodynamic characterization of nickel metal foam, part 1: single-phase permeability. Transp. Porous Media **80**(2), 269–279 (2009)
Mota, M., Teixeira, J., Yelshin, A.: Image analysis of packed beds of spherical particles of different sizes. Sep. Purif. Technol. **15**(1-4), 59–68 (1999)
Nałęcz, T.: Laboratory of fluid mechanics—exercise. ART Publishing House, Olsztyn (1991) (in Polish)
Neethirajan, S., Karunakaran, C., Jayas, D.S., White, N.D.G.: X-Ray computed tomography image analysis to explain the airflow resistance differences in grain bulks. Biosyst. Eng. **94**(4), 545–555 (2006)
Neithalath, N., Weiss, J., Olek, J.: Predicting the permeability of pervious concrete (enhanced porosity concrete) from non-destructive electrical measurements. Available at https://fp.auburn.edu/heinmic/perviousconcrete/Porosity.pdf Accessed 5 October 2009
Niven, R.K.: Physical insight into the Ergun and Wen & Yu equations for fluid flow in packed and fluidised beds. Chem. Eng. Sci. **57**(3), 527–534 (2002)
Pazdro, Z., Bohdan, K.: General Hydrogeology. Geological Publisher, Warsaw (1990) (in Polish)
Perret, J.S., Prasher, O., Kantzas, A., Langford, C.: Three-dimensional quantification of macropore networks in undisturbed soil cores. Soil Sci. Soc. Am. J. **63**(6), 1530–1543 (1999)
Samsuri, A., Sim, S.H., Tan, C.H.: An integrated sand control method evaluation. Society of Petroleum Engineers, SPE Asia Pacific Oil and Gas Conference and Exhibition, Jakarta, Indonesia, 9–11 September (2003)
Sawicki, J., Szpakowski, W., Weinerowska, K., Woloszyn, E., Zima, P.: Laboratory of fluid mechanics and hydraulics. Gdansk University of Technology, Gdansk, Poland (2004) (in Polish)
Skjetne, E., Klov, T., Gudmundsson, J.S.: High-velocity pressure loss in sandstone fractures: modeling and experiments (SCA-9927, 12 pp.). In: International Symposium of the Society of Core Analysts, Colorado School of Mines, Colorado, August 1–4 1999
Sobieski, W.: Switch function and sphericity coefficient in the gidaspow drag model for modeling solid-fluid systems. DRYING TECHNOLOGY **27**(2), 267–280 (2009). ISSN 0737-3937
Tavarez, F.A., Plesha, M.E.: Discrete element method for modelling solid and particulate materials. Int. J. Numer. Methods Eng. **70**, 379–404 (2007)
Wu, J., Yu, B., Yun, M.: A resistance model for flow through porous media. Transp. Porous Media **71**(3), 331–343 (2008)
Yu, B.M., Li, J.H.: A geometry model for tortuosity of flow path in porous media. Chin. Phys. Lett. **21**(8), 1569–1571 (2004)
Yun, M.J., Yu, B.M., Zhang, B., Huang, M.T.: A geometry model for tortuosity of streamtubes in porous media with spherical particles. Chin. Phys. Lett. **22**(6), 1464–1467 (2005)